Turbulent Reacting Flow Simulation Based on the Multi-Environment Mixing Model*

O. MIERKA, J. STOPKA**, M. KIŠA, and Ľ. JELEMENSKÝ

Department of Chemical and Biochemical Engineering, Faculty of Chemical and Food Technology, Slovak University of Technology, SK-812 37 Bratislava
e-mail: jan.stopka@stuba.sk

Received 1 April 2005

In this work a CFD approach is described for modelling fast chemical reactions in turbulent liquid flows. The relevant model developed for this purpose is composed of a core for the solution of Navier—Stokes equations and extended with an appropriate turbulence model. Treatment of additional (passive or active) scalars is performed on the basis of velocity fields obtained by means of a "hydrodynamic core engine". The developed CFD model was benchmarked on the so-called backward-facing step problem and reasonably correlated with the values reported.

The turbulence model used to simulate micromixing phenomena was derived from the scalar dissipation rate, which is obtained from the turbulent kinetic energy and its dissipation. For this purpose, a multi-environment mixing model was developed. This model enables modelling of the flow of nonpremixed environments of liquid phases, where chemical reactions do not occur, and also the flow of environments with different reaction rates due to different temperatures and concentrations of species involved.

Generally, in the case of modelling of N environments and S chemical species, the use of such micromixing approach means evaluation of $N+(N-2)\,S+N-1$ additional scalar fields of individual environments, temperatures, and species in these environments.

As a reaction system, a commonly used set of competitive-consecutive reactions ($A + B \rightarrow 2P$ $A + P \rightarrow 2R$) occurring in a triple-jet channel reactor was considered. Simulations were executed in 2D. Their results, however, need validation by experimental data.

Transport of species, momentum, and energy is much faster in a turbulent regime of flow by molecular diffusion. This is the reason, why chemical process industry prefers rather these conditions than a laminar regime. Mixing is also an important phenomenon apart from considered hydrodynamic conditions within the equipment (*e.g.* a reactor or combustor). Thus, it is obvious that simulation of a process, taking place in such equipment is based on superposition of both hydrodynamics and mixing on all scales (including micro- and macromixing of all scalar variables).

The coupled system of differential equations describing the flow consists of Reynolds Averaged Navier—Stokes equations and $k-\varepsilon$ equations, which could be treated in a cascade of two nonlinear iteration cycles (k is the turbulent kinetic energy and ε is its dissipation). In this study, the cycle of coupled $k-\varepsilon$ equations with implicit sources was nested in an outer nonlinear cycle of Navier—Stokes equations based on calculated and updated turbulent viscosities [1, 2]. Calculation of "isolated" variables was then handled in defect-correction loops including stabilization of the convective terms. In this work, the stabilization is based on an appropriate advection algorithm, proposed within the framework of the total variation diminishing (TVD) method [1].

The method used to solve a mixing phenomenon is not as straightforward as it was described for the flow motion. First studies dealing with such modelling stretch back to 1976, when the Eddy Dissipation Concept (EDC) was developed [3]. Here, the solution was obtained by means of two types of variables, namely the volume fraction of species and the mixture fraction. Then, the transport equations for the conserved volume fraction of species were solved using limited reaction rates reflecting the magnitude of mixing.

A more sophisticated method, taking into account various scales of mixing, was reported by *Baldyga* [4], who specified the multiple-time-scale (MTS) turbu-

*Presented at the 32nd International Conference of the Slovak Society of Chemical Engineering, Tatranské Matliare, 23—27 May 2005.

**The author to whom the correspondence should be addressed.

lent mixer model. This model aspired to express the inertial-convective, viscous-convective, and viscous-diffusive scales of mixing and their overall contribution to the mixing. Recently this model had its substantiation [5]. Even though, nowadays the effort is focused on the probability density function (PDF) method. This method attributes to individual scalars (*e.g.* the volume fraction of species or the temperature) a new dimension, which expresses the probability of mixedness of the surrounding fluid. Essentially, the multi-environment micromixing model (MEMM) described here is the multi-environment presumed PDF model with no reaction occurring in the 1st or the *N*-th environment. By means of this method, the scalar variables dependent on the micromixing are discretized to a finite number of environments between which the exchange of material and energy is governed by probability fluxes [6—8]. Then, for these probability fluxes the corresponding parameters based on the Eulerian mixing time should be estimated [6].

The goal of the work is to give an integrated insight into both approaches, the simulation of the flow and the reaction system, and outline the implementation technique. The CFD codes developed for simulation of reactive flows are referenced exclusively to commercial software, where the additional features enabling the simulation of reactive flows are carried out by user-defined functions. By the present work and the provided references the creation of simulation software is enabled for reactor engineering purposes constrained to incompressible liquid flows.

THEORETICAL

The hydrodynamic engine solves the RANS equations coupled with the $k-\varepsilon$ equations, which are also mutually coupled. The system of the governing differential equations is defined as follows

$$\frac{\partial \mathbf{u}}{\partial t} + \mathbf{u}\cdot\nabla\mathbf{u} - \nabla\cdot\left\{-\left(p+\frac{2}{3}k\right)\mathbf{I} + (\nu_{\mathrm{turb}}+\nu)\left[\nabla\mathbf{u}+(\nabla\mathbf{u})^{\mathrm{T}}\right]\right\} = \mathbf{f} \qquad (1)$$

$$\nabla\cdot\mathbf{u} = 0 \qquad (2)$$

$$\frac{\partial k}{\partial t} + \nabla\cdot(k\,\mathbf{u} - d_k\nabla k) + \gamma_{k-\varepsilon}\,k = P_k \qquad (3)$$

$$\frac{\partial \varepsilon}{\partial t} + \nabla\cdot(\varepsilon\mathbf{u} - d_\varepsilon\nabla\varepsilon) + C_2\,\gamma_{k-\varepsilon}\,\varepsilon = C_1\gamma_{k-\varepsilon}\,P_k \qquad (4)$$

where

$$p = \frac{P^{\mathrm{pressure}}}{\rho} \qquad d_k = \frac{\nu_{\mathrm{turb}}}{\sigma_k} + \nu$$
$$d_\varepsilon = \frac{\nu_{\mathrm{turb}}}{\sigma_\varepsilon} + \nu \qquad (5)$$
$$\gamma_{k-\varepsilon} = \frac{\varepsilon}{k}\nu_{\mathrm{turb}} = c_\mu\frac{k^2}{\varepsilon}$$

$$P_k = \frac{\nu_{\mathrm{turb}}}{2}\left|\nabla\mathbf{u} + (\nabla\mathbf{u})^{\mathrm{T}}\right|^2 \qquad (6)$$

with the following parameters values: $c_\mu = 0.09,\ C_1 = 1.44,\ C_2 = 1.92,\ \sigma_k = 1.0$, and $\sigma_\varepsilon = 1.3$.

It is important to remark that the equations of k and ε are strongly coupled and therefore, the computation is nonlinear. Furthermore, diffusion, reaction, and source terms are nonnegative for nonnegative initial conditions of both scalar variables, which implies that their discretization has to be positivity-preservation. Eqns (*3*) and (*4*) are written according to the representation proposed in [2]. The author found that for the positivity-preservation more important is the positivity of the lagged coefficients, *i.e.* the negative values of k and ε. Generally, this concept is based on the limitation of the mixing length, turbulent eddy viscosity, and turbulent kinetic energy in the individual defect-correction steps (see [1]). Considering positivity-preservation, discretization of the convective terms is suitable to perform with the TVD technique [1], which guarantees positivity of the converged values and not that of the intermediate solution values.

For the velocity $\mathbf{n}\cdot\mathbf{u} = 0$, in addition to the inflow and outflow conditions, also the no-penetration wall function condition is imposed, as originally proposed by *Launder* and *Spalding* [11]. This internal boundary condition is imposed at a distance δ from the solid wall, Γ_δ, taking into account the fact that the computational domain is reduced by width of the boundary layer δ

$$\left\{(\nu_{\mathrm{turb}}+\nu)\left[\nabla\mathbf{u}+(\nabla\mathbf{u})^{\mathrm{T}}\right]\right\}\cdot\mathbf{t} = -u_\tau^2\frac{\mathbf{u}}{|\mathbf{u}|} \qquad (7)$$

at the solid wall, Γ_δ. In eqn (*7*) u_τ is the friction velocity, which is defined by the following relationship

$$|\mathbf{u}| - u_\tau\left(\frac{1}{\kappa}\log y^+ + 5.5\right) = 0 \qquad (8)$$

for $20 \le y^+ \le 100$.

Since this boundary condition is implicit with respect to the friction velocity, it is solved iteratively by the Newton's method. For y^+ it holds

$$y^+ = \frac{u_\tau\delta}{\nu} \qquad (9)$$

within the range $20 \le y^+ \le 100$, and

$$u_\tau = \sqrt{\frac{\nu\,|\mathbf{u}|}{\delta}} \qquad (10)$$

for $y^+ < 20$.

At the solid wall, Γ_δ, the empirical boundary conditions for k and ε are the following

$$k = \frac{u_\tau^2}{\sqrt{c_\mu}} \qquad \varepsilon = \frac{u_\tau^3}{\kappa\,\delta} \qquad (11)$$

It should be noted that eqns (*7*—*11*) represent the standard wall function [11].

For the inflow and outflow the values for $\mathbf{u}$, k, and ε are given by the following

$$\mathbf{u} = \mathbf{g} \quad k = c_{\mathrm{bc}} |\mathbf{u}|^2 \quad \varepsilon = c_\mu \frac{k^{3/2}}{l_0} \quad \text{at } \Gamma_{\mathrm{inflow}} \tag{12}$$

$$\mathbf{n} \cdot \left\{ -\left(p + \frac{2}{3}k\right)\mathbf{I} + (\nu_{\mathrm{turb}} + \nu)\left[\nabla\mathbf{u} + (\nabla\mathbf{u})^{\mathrm{T}}\right]\right\} = 0$$

$$\mathbf{n} \cdot \nabla\varepsilon = 0 \qquad \mathbf{n} \cdot \nabla k = 0 \qquad \text{at } \Gamma_{\mathrm{outflow}} \tag{13}$$

which reflects the fact that in most cases the simulations of unsteady flows are initiated from motionless state, where no turbulence is present. The approach used here (corresponding to [1]) is based on a two-stage simulation. In the first stage, which can be characterized as a laminar flow, the turbulence transport equations are not computed. After reaching a certain time $t_{k-\varepsilon}$ during this laminar computation the turbulence variables are initiated by the following equations

$$k_0 = \left(\frac{\nu_0}{l_0}\right)^2 \qquad \varepsilon_0 = c_\mu \frac{k^{3/2}}{l_0} \qquad \text{at } t = t_{k-\varepsilon} \tag{14}$$

Then, the time $t_{k-\varepsilon}$ is characterized as the initial time for the turbulence variables computation and consequently, for the second stage of the modelling of flow.

Micromixing defined by the MEMM approach requires modelling of the individual environments and estimation of the volume fraction of individual species in all these environments. In general, if N is the number of environments and S is the number of species a coupled system of additional $N+N.S+N$ scalar transport equations (N for environments, $N.S$ for species, and N for temperatures) is considered. The final number of equations will be adjusted at the end of the description of the model. The above-mentioned transport equations will be expressed in terms of $p_i(\mathbf{x}, t)$ and $s_\alpha^{(i)}(\mathbf{x}, t)$ in order to satisfy the conservation of probability. Each environment corresponds to a discretization of the composition PDF in a finite set of delta functions

$$f_\varphi(\boldsymbol{\psi}; \mathbf{x}, t) = \sum_{i=1}^{N} p_i(\mathbf{x}, t) \left[\prod_{\alpha=1}^{S} \zeta\left(\psi_\alpha - \phi_\alpha^{(i)}(\mathbf{x}, t)\right)\right] \tag{15}$$

where the product takes into account all species and the sum considers all environments. Then, the transport equations are as follows

$$\frac{\partial p_i}{\partial t} + \mathbf{u} \cdot \nabla p_i = \nabla \cdot (d_{\mathrm{turb}} \nabla p_i) + G_i(\mathbf{p}) \tag{16}$$

$$\frac{\partial s_\alpha^{(i)}}{\partial t} + \mathbf{u} \cdot \nabla s_\alpha^{(i)} = \nabla \cdot \left(d_{\mathrm{turb}} \nabla s_\alpha^{(i)}\right) + M_\alpha^{(i)}\left(\mathbf{p}, \mathbf{s}^{(n)}\right) + p_i S_\alpha\left(\boldsymbol{\varphi}^{(i)}\right) \tag{17}$$

where $G_i(\mathbf{p})$ and $M_\alpha^{(i)}\left(\mathbf{p}, \mathbf{s}^{(n)}\right)$ are the micromixing functions defined in terms of probability fluxes r_i. Summation of these terms over all environments has to be equal to zero, because these source terms are responsible just for the exchange of mass between the environments. Thus, they cannot affect the global conservation of mass. Definition of probability fluxes, for four environments is presented below

$$\begin{aligned} r_1 &= \gamma p_1 (1 - p_1) \\ r_2 &= \gamma p_2 \\ r_3 &= \gamma p_3 \\ r_4 &= \gamma p_4 (1 - p_4) \end{aligned} \tag{18}$$

The rate of micromixing, γ, can be computed as a function of k and ε (*Hjertager* [13])

$$\gamma = C_\phi \frac{\varepsilon}{k} \tag{19}$$

The value of C_ϕ depends on the state of turbulence development. The value of this parameter varies within the range of $\langle 0.5, 1.0 \rangle$ (see [7] and [13]), where the value of 1.0 is assumed in the case of developed turbulence, and the value of 0.5 is proposed in regions where erosion of the velocity field takes place (injection points).

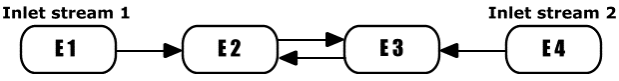

Fig. 1. Mass balance with respect to the micromixing fluxes for 4 environments.

Then, based on the mass balance shown in Fig. 1, the micromixing functions are defined as follows

$$\begin{aligned} G_1 &= -r_1 \\ G_2 &= +r_1 - r_2 + r_3 \\ G_3 &= +r_2 - r_3 + r_4 \\ G_4 &= -r_4 \end{aligned} \tag{20}$$

$$\begin{aligned} \mathbf{M}_\alpha^{(1)} &= -r_1\boldsymbol{\varphi}_\alpha^{(1)} \\ \mathbf{M}_\alpha^{(2)} &= +r_1\boldsymbol{\varphi}_\alpha^{(1)} - r_2\boldsymbol{\varphi}_\alpha^{(2)} + r_3\boldsymbol{\varphi}_\alpha^{(3)} \\ \mathbf{M}_\alpha^{(3)} &= +r_2\boldsymbol{\varphi}_\alpha^{(2)} - r_3\boldsymbol{\varphi}_\alpha^{(3)} + r_4\boldsymbol{\varphi}_\alpha^{(4)} \\ \mathbf{M}_\alpha^{(4)} &= -r_4\boldsymbol{\varphi}_\alpha^{(4)} \end{aligned} \tag{21}$$

The definition of the micromixing terms by eqns (*20*) and (*21*) neglects the effect of the terms used to eliminate the so-called spurious dissipation. This assumption is based on the work reported by *Piton et al.* [12], who modelled a tubular reactor. For the relationship between the volume fraction of species α in the environment i, $s_\alpha^{(i)}$, and the local concentration of this

scalar variable, $\varphi_\alpha^{(i)}$, and its mean value, $\varphi_\alpha = \sum_{i=1}^{N} s_\alpha^{(i)}$, the following equation holds

$$\varphi_\alpha^{(i)} = \frac{s_\alpha^{(i)}}{p_i} \qquad i = 2,\ 3,\ 4 \tag{22}$$

Starting from eqns (*16*) and (*17*), omitting the source term, S_1, and defining $\xi = \varphi_1$, the mixture fraction variance ξ'^2 could be computed from the equation

$$\xi'^2 = \sum_{i=1}^{N} \frac{\left(s^{(i)}\right)^2}{p_i} - \xi^2 \tag{23}$$

Application of the MEMM for reacting flows does not affect only the composition but also the temperature field, which means modelling of N temperature fields for each individual environment. The exchange of heat between the neighbouring cells is also defined by the same probability fluxes as in the case of the volume fractions. The "temperature probabilities" are calculated in the environments by means of the following transport equation

$$\begin{aligned} &\frac{\partial \tau^{(i)}}{\partial t} + \mathbf{u} \cdot \nabla \tau^{(i)} = \\ &\nabla \cdot \left(a_{\mathrm{turb}} \nabla \tau^{(i)} \right) + O^{(i)}\left(\mathbf{p}, \mathbf{T}\right) + p_i\, Q^i\left(T^{(i)}\right) \\ &\text{for} \quad i = 1,\ \ldots\ N \end{aligned} \tag{24}$$

This transport equation is written for the product of the temperature $T^{(i)}$ and the environmental fraction p_i in the given environment i. In eqn (*24*) $O^{(i)}\left(\mathbf{p}, \mathbf{T}\right)$ is the contribution of the micromixing source term and its definition is as follows

$$\begin{aligned} O_\alpha^{(1)} &= -\, r_1 T_\alpha^{(1)} \\ O_\alpha^{(2)} &= +\, r_1 T_\alpha^{(1)} - r_2 T_\alpha^{(2)} + r_3 T_\alpha^{(3)} \\ O_\alpha^{(3)} &= \qquad + r_2 T_\alpha^{(2)} - r_3 T_\alpha^{(3)} + r_4 T_\alpha^{(4)} \\ O_\alpha^{(4)} &= \qquad\qquad\qquad - r_4 T_\alpha^{(4)} \end{aligned} \tag{25}$$

Then, the mean local temperature is calculated from the following equation

$$T = \sum_{i=1}^{N} p_i T^{(i)} = \sum_{i=1}^{N} \tau^{(i)} \tag{26}$$

For the reactive flows in eqn (*24*) the term $p_i\, Q^i\left(T^{(i)}\right)$ expresses the contribution of the released reaction heat multiplied with the environmental fraction for the given environment. Its definition depends on the kinetics of the reaction.

Calculation of all "environmental" scalars at non-reactive flow conditions should satisfy the overall conservation of given variable. For this reason, it is necessary to check the sum for all of these variables and implement a suitable mechanism to satisfy the mean scalar conservation requirement. For the environmental fraction this mechanism is implemented by means of renormalization, *i.e.*

$$p_j^{\mathrm{l}+1} = \frac{p_j^{\mathrm{l}}}{\sum\limits_{i}^{N} p_i^{\mathrm{l}}} \tag{27}$$

where l+1 represents the updated environmental fraction values. For the volume fraction of species the renormalization is calculated as follows

$$s_j^{\alpha,\mathrm{l}+1} = \frac{s_j^{\beta,\mathrm{l}} p_j^{\mathrm{l}+1}}{\sum\limits_{\beta=1}^{S} s_j^{\beta,\mathrm{l}}} \tag{28}$$

The temperature cannot be treated directly in that manner as the previous scalars. However, because the micromixing fluxes for these variables cancel out in case of summing up all the N transport equations, it is possible to calculate the mean temperature $\langle T \rangle$. The source term in this newly introduced additional scalar equation is formed exclusively by the environmental chemical production terms. Then, the mean temperature calculated in this way is used in the renormalization computation as

$$\tau_j^{\mathrm{l}+1} = \frac{\tau_j^{\mathrm{l}} \langle T \rangle}{\sum\limits_{i}^{N} \tau_i^{\mathrm{l}}} \tag{29}$$

Since neither influence of temperature nor effect of concentration of species on the density or viscosity was assumed, hydrodynamic calculations could be implemented separately from the micromixing-based scalar variables. Such an assumption leads to the calculation algorithm outlined in Fig. 2. According to this scheme, the $k-\varepsilon$ equations are inserted after the nonlinear computation of the velocity components. As the convergence criterion of the outer iteration cycle the norm of relative changes and the norm of defects of the velocity components were utilized.

Now, let us go back to the determination of the final number of equations subjected to simulation within the MEMM framework. Taking into account that there are not other species present in the 1st (N-th) environment except species A (B), and the volume fraction of species A (B) is therefore equal to the volume fraction of this 1st (N-th) environment, the number of equations decreases to $N + (N-2)\ S + N$. The fact that the "environmental" temperatures of the 1st and N-th environment are calculated directly by the environmental fractions of these environments modifies the number of equations to $N + (N-2)\ S + N - 2$. We can see that this number finally increased by one

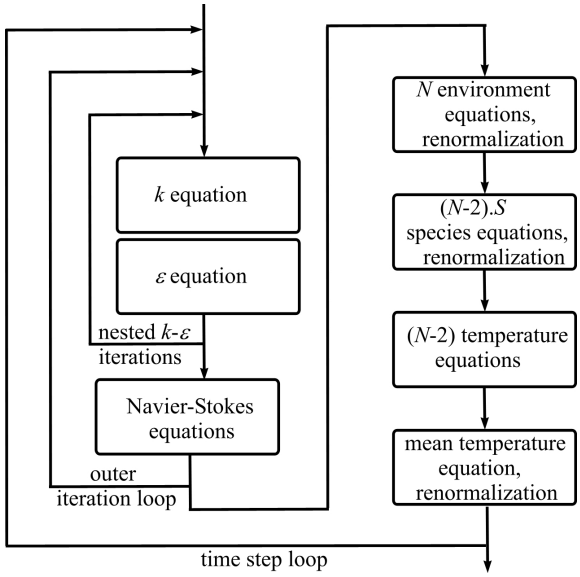

Fig. 2. The sketch of the calculation algorithm.

(Fig. 2), because of the calculation of the mean temperature required for the temperature renormalization.

On the contrary to other standard approaches [6, 8] the algorithm presented here takes into account the calculation of all nonzero environmental fractions and the volume fractions of species. In this way, none of the variables is calculated by subtraction from unity. Thus, a potential source of accumulation of a numerical error is avoided.

RESULTS AND DISCUSSION

As mentioned above, the development of the micromixing model requires first of all a hydrodynamic engine, which provides the fields of the turbulent kinetic energy k and its dissipation ε. In this work the upgraded FEATFLOW program was used for this purpose. The program was tested on a benchmark problem with the aim to validate the turbulence model. The chosen benchmark was the same as that used by some other research groups [1, 9, 14—16]. This benchmark corresponds to the so-called "backward-facing step". The geometry of this problem is shown in Fig. 3, in which also the boundary conditions are given. The characteristic Reynolds number for this benchmark computation is based on the characteristic length H and the mean upstream velocity v_0, and is equal to 44000. Then, justification of the hydrodynamic solver is obtained from comparisons of several chosen variable distributions with those reported by other researchers and from the length of the recirculation zone, which is predicted to be 7.1 H [15] for the given benchmark computation.

The results of simulation obtained at steady-state conditions are presented in Table 1. In order to obtain

Fig. 3. Problem description of the backward-facing step.

Table 1. Calculated Recirculation Lengths for the Two Different Meshes, TVD Limiters (MC and Superbee), Boundary Layer Distances ($\delta = 0.050$ and 0.025), and Mesh Levels 4—7*

δ	Limiter	Mesh level	x_r 1st mesh	x_r 2nd mesh
0.050	MC	4	5.47	6.16
		5	6.47	6.88
		6	6.87	7.19
		7	–	7.29*
	SB	4	5.28	6.03
		5	6.27	6.72
		6	6.74	7.05
0.025	MC	4	5.7	6.34
		5	6.78	7.09
		6	7.14	7.36

*Result from UNI-Dortmund/Department of Applied Mathematics. δ – width of the boundary layer, x_r – length of the recirculation zone.

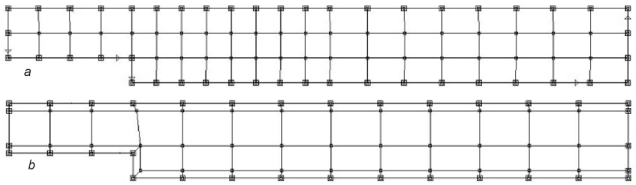

Fig. 4. Two different coarse meshes used for the investigation of mesh independence.

mesh-independent solution profiles two coarse meshes were used (Fig. 4) with three/four subsequent multigrid levels (4—7). Additionally, the calculations were performed with two different TVD limiters (MC and Superbee) for the following values of parameters: $\delta = 0.05$ and 0.025, $c_{bc} = 0.025$, $\nu_0 = 10^{-3}$, $l_0 = 0.02$, and $l_{max} = 1.0$.

The length of the recirculation zone was calculated by means of the streamline field, where the length of the "last" streamline belonging to the recirculation was measured. A brief summary of the performed simulations with respect to the recirculation zone is listed in Table 1. The parameters, for which the recirculation length was calculated, are also explained in the caption to this table. In Table 2 are presented the numbers of generated elements for the two coarse meshes depending on the considered multi-grid com-

Table 2. Number of Elements Generated for the Two Coarse Meshes with Respect to the Multi-Grid Level Considered

Multi-grid level	Number of elements for the 1st mesh	Number of elements for the 2nd mesh
4	3584	3200
5	14336	12800
6	57344	51200
7	–	204800*

*Mesh generated by UNI-Dortmund/Department of Applied Mathematics.

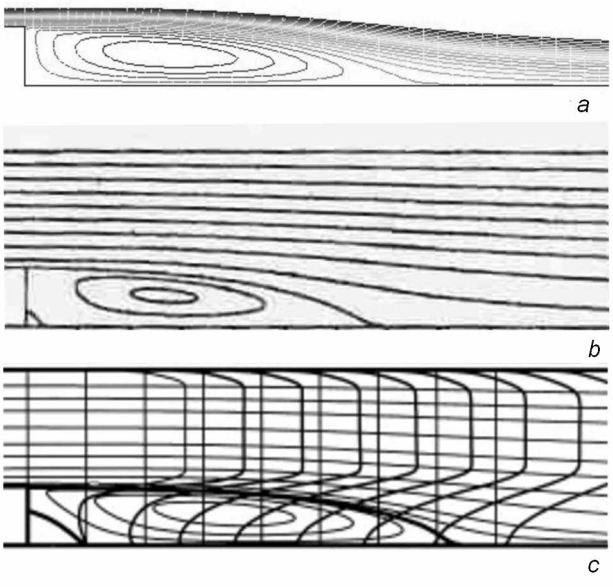

Fig. 5. Streamlines for the backward-facing step for Re = 44000. *a*) FEATFLOW calculated, *b*) calculated with anisotropic viscosity with relative error within 3 % [15], *c*) calculated by high-Re number model with wall functions [16].

putation level. The comparison of the calculated fields for steady state is based on the streamlines (Fig. 5*a*), distribution of the turbulent kinetic energy and turbulent viscosity (Figs. 7*a* and *c*) with the same variable distributions published for the given benchmark (Figs. 5*b* and *c* for the streamlines and Figs. 7*b* and *d* for the turbulent kinetic energy and turbulent viscosity) [1, 9, 14, 15]. A supplemental comparison with the presented reference data was carried out by means of the streamline velocity profiles at the distance of 5.33 H from the step corresponding to that given by *Kim et al.* [14] (Fig. 6). As far as a very good agreement was found with the presented references, the modified FEATFLOW program proved to be useful in simulations of Reynolds Averaged Navier—Stokes equations.

The second task of this work is the testing of the MEMM approach. Prior to the simulation of the turbulent reactive incompressible flow, the micromixing

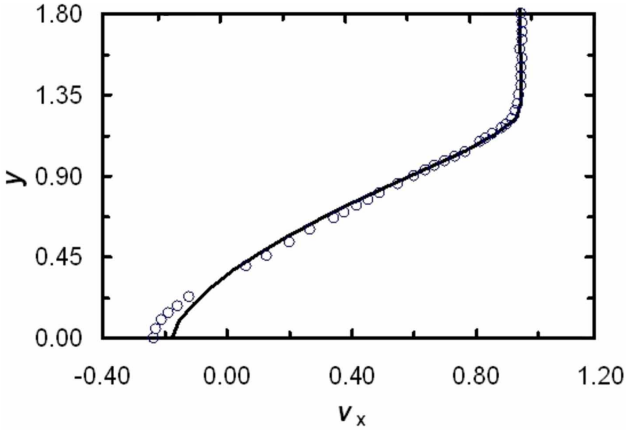

Fig. 6. Streamline velocity components distribution at the position 5.33 H from the step for Re = 44000. ○ Experimental [14], — FEATFLOW calculated.

model was validated for the case of mixing of two material streams, for which the justness and the accuracy of the output stream can be verified [10]. For this reason, mixing of two inflow streams between two infinitely wide and long plates (see Fig. 8*a*) was simulated with chemical reactions. In Fig. 8*b* is given the generated coarse mesh for this 2D problem. Then, the computation was based on the multi-grid approach up to the fifth level, what involves the generation of 17408 elements. Corresponding to Fig. 8*b*, stricter size requirements were placed on the elements in the vicinity of the mixing region of the inflowing streams. The highest applied fifth multi-grid level proved to be high enough to provide results with a satisfactory mesh-independent property. This fact can be mostly expressed *via* the fifth multi-grid level distribution of ε projected to the fourth level mesh (see Fig. 9*a*). From the mentioned figure it can be seen that the one level lower (fourth) generated mesh is also able to resolute the steep distribution of this chosen variable in the critical region.

The velocity boundary conditions for this reactive flow problem were applied by the following way

$$\frac{v_x^{\text{1st stream}}}{v_x^{\text{2nd stream}}} = \frac{2}{1} \qquad (30)$$

in order to ensure that the volumetric flow of both streams was equal. The Reynolds number for this problem, based on the characteristic length H and streamline velocity $v_x^{\text{2nd stream}}$, was 99000. The calculated steady-state velocity profile for this problem is presented in Fig. 9*c* and the distribution of the micromixing rate, γ, derived from the turbulent kinetic energy and its dissipation is presented in Fig. 9*b*. The figure reveals that this variable has also a very steep distribution in the region, where the feeds are introduced. Thus, the generation of an appropriate coarse mesh for the upcoming MEMM calculation was almost essential.

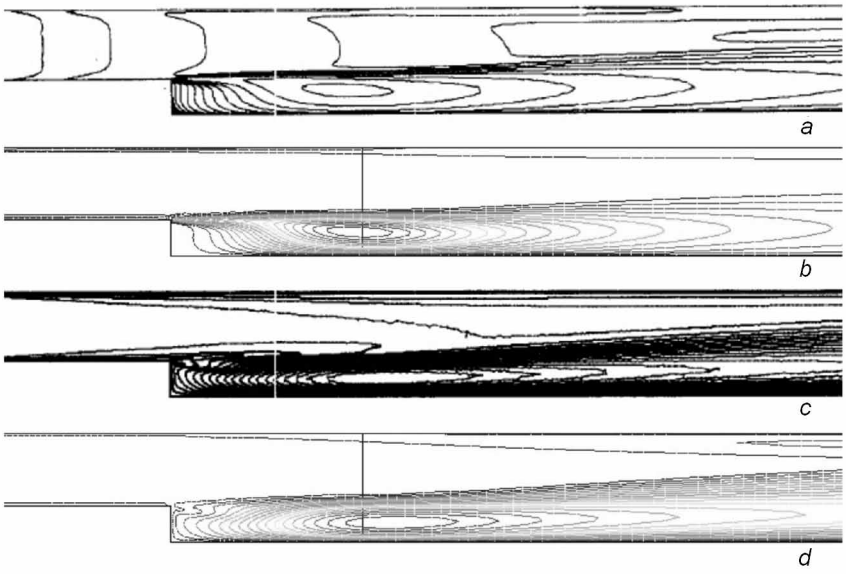

Fig. 7. Distribution of the turbulent kinetic energy (a and b) and turbulent viscosity (c and d) for $Re = 44000$. b) and d) are experimental data measured by *Ilinca et al.* [17] and a) and c) are FEATFLOW calculated values.

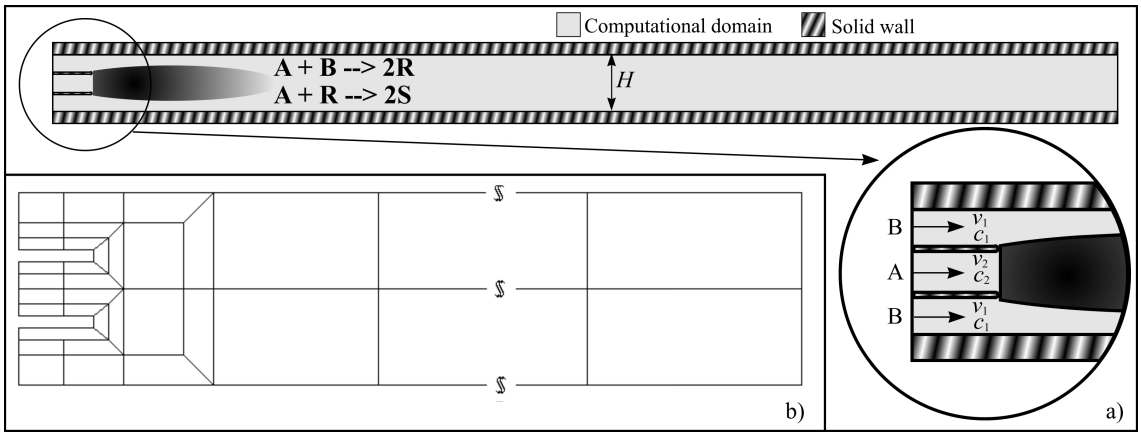

Fig. 8. Problem description of the 2D mixing channel. a) Geometry of the computational domain and the configuration of the streams, b) the used coarse mesh.

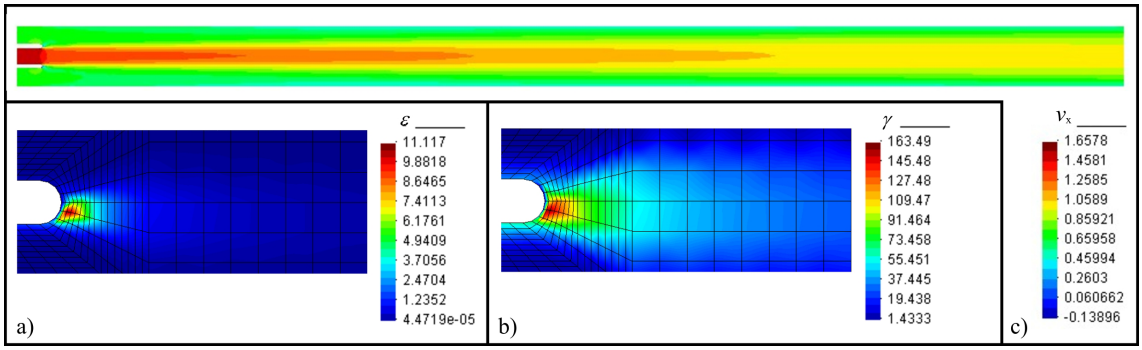

Fig. 9. Distribution of: a) dissipation of turbulent kinetic energy ε in the mixing region, b) micromixing rate function γ in the mixing region; at steady-state regime for reacting flow, c) streamline velocity component v_x.

Finally, a reacting system comprising the following consecutive-competitive reaction schemes

$$\mathrm{A} + \mathrm{B} \rightarrow 2\mathrm{P} \qquad (A)$$

$$A + P \rightarrow 2R \qquad (B)$$

was investigated. It was assumed that the pre-exponential value in the Arrhenius-defined reaction

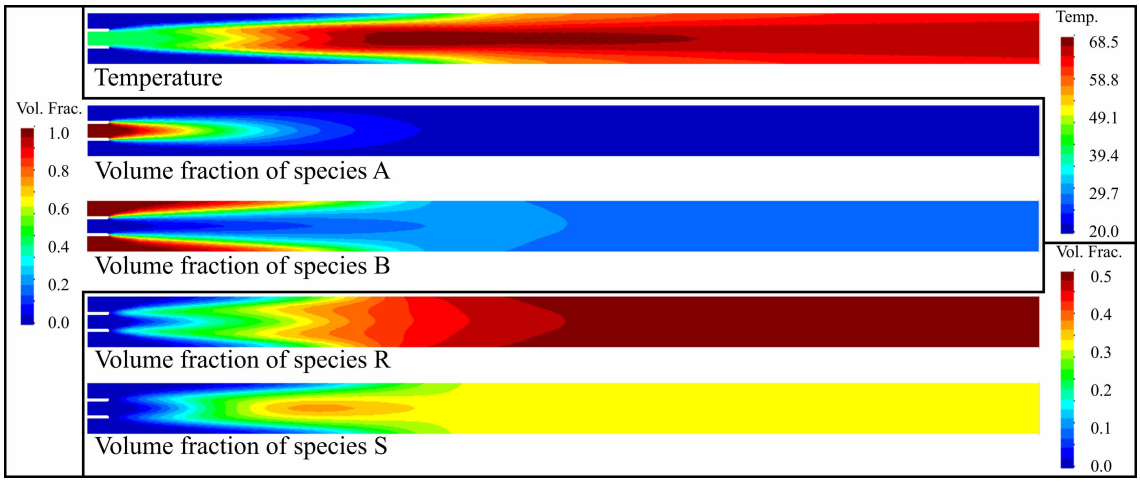

Fig. 10. Distribution of temperature and volume fractions of species at steady-state regime for reacting flow in a 2D channel reactor.

rate for reaction (B) was 10 times smaller than the pre-exponential factor of the reaction (A). The dependence of physicochemical properties on the temperature was not taken into account for this model system. However, in case of modelling real problems, the effect of these dependences should not be neglected. As shown in Fig. 10, chemical reactions occur in the first half of the planar triple-jet reactor and reach a steady vertical profile in the second half of the reactor. Finally, the authors of this work would like to stress that the presented results (corresponding to the turbulent reactive flow) were obtained for a model system and were not compared with experimental data. For this reason they should be considered with an adequate reserve.

Acknowledgements. This work was supported by the Slovak Scientific Grant Agency. Grant No. VEGA 1/1377/04.

SYMBOLS

C	constant, parameter
d	diffusion coefficient, thermal diffusivity
$\mathbf{f}$	right-hand side (0 for incompressible flows)
$\mathbf{g}$	prescribed boundary value
k	turbulent kinetic energy
l	length
$\mathbf{M}$	micromixing production term
$\mathbf{n}$	normal vector
N	number of environments
$\mathbf{O}$	micromixing production term for the temperature
$\mathbf{p}$	environment probability vector
P^{pressure}	pressure
p	density divided by pressure
P	production term
$\mathbf{r}$	probability flux vector
Re	Reynolds number
$\mathbf{s}$	volume weighted fraction of species in a given environment
S	number of species
$\mathbf{S}$	chemical reaction production term
t	time
$\mathbf{t}$	unit vector
$\mathbf{T}$	environment temperature
$\langle T \rangle$	mean temperature
$\mathbf{u}$	velocity
y^+	wall distance

Greek Letters

δ	width of the boundary layer
ε	dissipation of the turbulent kinetic energy
$\boldsymbol{\varphi}$	volume fraction of species in a given environment
γ	rate of micromixing
$\gamma_{k-\varepsilon}$	ratio of ε to k
κ	von Kármán constant
ν	kinematic viscosity
ρ	density
τ	volume weighted temperature
ξ'^2	mixture fraction variance
ζ	Dirac delta function

Subscripts

0	initial
α, β	species
i, j	environment
turb	turbulent variable
τ	shear stress

Superscripts

(i)	environment index
l	iteration index
T	transposed

REFERENCES

1. Kuzmin, D., Löhner, R., and Turek, S., *Flux-Corrected Transport*, p. 301. Springer, Berlin, 2005.
2. Lew, A. J., Buscaglia, G. C., and Carrica, P. M., *Int. J. Comput. Fluid Dynam. 14*, 201 (2001).
3. Magnussen, B. F. and Hjertager, B. H., *On mathematical modelling of turbulent combustion with special emphasis on soot formation and combustion.* In *16th International Symposium on Combustion*, Pittsburgh, 1976.
4. Baldyga, J., *Chem. Eng. Sci. 44*, 1175 (1989).
5. Hjertager, L. K., Hjertager, B. H., and Solberg, T., *Comput. Chem. Eng. 26*, 507 (2002).
6. Fox, R. O., *Chem. Eng. Proc. 37*, 521 (1998).
7. Kolhapure, N. H. and Fox, R. O., *Chem. Eng. Sci. 54*, 3233 (1999).
8. Wang, L. and Fox, R. O., *AIChE J. 50*, 2217 (2004).
9. Medić, G. and Mohammadi, B., *NSIKE – an incompressible Navier—Stokes solver for unstructured meshes*, Internal Report, p. 66. Le Chesnay, 1999.
10. Mierka, O., Stopka, J., Kiša, M., and Jelemenský, Ľ., *Multi-environment micromixing model comparisons for reactive flows.* In *32nd International Conference of SSCHE*, Tatranské Matliare, Slovakia, 2005.
11. Launder, B. E. and Spalding, D. B., *Comp. Methods Appl. Mech. Eng. 3*, 269 (1974).
12. Piton, D., Fox, R. O., and Marcant, B., *Can. J. Chem. Eng. 78*, 983 (2004).
13. Hjertager, L. K., *PhD. Thesis.* Aalborg University, Esbjerg, 2004.
14. Kim, J., Kline, S. J., and Johnston, J. P., *Fluids Eng. 102*, 302 (1980).
15. Thangam, S. and Speziale, C. G., *AIAA J. 30*, 1314 (1992).
16. Hanjalić, K. and Jakirlić, S., *Comput. Fluids 27*, 137 (1998).
17. Ilinca, F., Hétu, J.-F., and Pelletier, D., *Comput. Fluids 27*, 291 (1998).